THE JOURNAL OF BIOLOGICAL CHEMISTRY VOL. 291, NO. 18, pp. 9776–9784, April 29, 2016

Bithionol Potently Inhibits Human Soluble Adenylyl Cyclase through Binding to the Allosteric Activator Site*

Received for publication, December 3, 2015, and in revised form, March 3, 2016 Published, JBC Papers in Press, March 9, 2016, DOI 10.1074/jbc.M115.708255

Silke Kleinboelting[‡1], Lavoisier Ramos-Espiritu[§¶], Hannes Buck[§], Laureen Colis[§], Joop van den Heuvel[‖], J. Fraser Glickman[¶], Lonny R. Levin[§], Jochen Buck[§], and Clemens Steegborn[‡2]

From the [‡]Department of Biochemistry, University of Bayreuth, 95440 Bayreuth, Germany, [§]Department of Pharmacology, Weill Cornell Medical College, New York, New York 10065, [¶]High Throughput Screening and Spectroscopy Resource Center, The Rockefeller University, New York, New York 10065, and [‖]Helmholtz-Zentrum für Infektionsforschung, 38124 Braunschweig, Germany

The signaling molecule cAMP regulates functions ranging from bacterial transcription to mammalian memory. In mammals, cAMP is synthesized by nine transmembrane adenylyl cyclases (ACs) and one soluble AC (sAC). Despite similarities in their catalytic domains, these ACs differ in regulation. Transmembrane ACs respond to G proteins, whereas sAC is uniquely activated by bicarbonate. Via bicarbonate regulation, sAC acts as a physiological sensor for pH/bicarbonate/CO_2, and it has been implicated as a therapeutic target, *e.g.* for diabetes, glaucoma, and a male contraceptive. Here we identify the bisphenols bithionol and hexachlorophene as potent, sAC-specific inhibitors. Inhibition appears mostly non-competitive with the substrate ATP, indicating that they act via an allosteric site. To analyze the interaction details, we solved a crystal structure of an sAC·bithionol complex. The structure reveals that the compounds are selective for sAC because they bind to the sAC-specific, allosteric binding site for the physiological activator bicarbonate. Structural comparison of the bithionol complex with apo-sAC and other sAC·ligand complexes along with mutagenesis experiments reveals an allosteric mechanism of inhibition; the compound induces rearrangements of substrate binding residues and of Arg^{176}, a trigger between the active site and allosteric site. Our results thus provide 1) novel insights into the communication between allosteric regulatory and active sites, 2) a novel mechanism for sAC inhibition, and 3) pharmacological compounds targeting this allosteric site and utilizing this mode of inhibition. These studies provide support for the future development of sAC-modulating drugs.

The universal second messenger cAMP regulates various cellular processes such as cell adhesion, gene expression, and energy metabolism (1, 2). In mammals, cAMP formation from ATP is catalyzed by two types of adenylyl cyclases (ACs),[3] nine transmembrane AC (tmAC) enzymes (AC1–9) and one soluble AC (sAC; AC10) (3). Mammalian sAC and tmAC both belong to nucleotidyl cyclase Class III, the largest of the six evolutionary distinct classes (2), and thus share a common catalytic core architecture (3). However, these ACs differ in their biological function and regulation. tmACs reside in the plasma membrane and are regulated by heterotrimeric G proteins in response to signals acting via G protein-coupled receptors. They thereby mediate cellular responses to extracellular signals. The nine tmAC isoforms show distinct tissue expression patterns and contribute to different physiological processes such as learning (AC1) and cardiac myocyte function (AC5) (4). sAC, in contrast, resides inside cells where it acts as an intracellular sensor for bicarbonate (HCO_3^-), ATP, and calcium (3). sAC is expressed in many tissues and can be found throughout the cytoplasm, inside the nucleus, and in mitochondria (3, 5). It contributes to functions such as sperm activation (6, 7), acid-base regulation (5, 8), astrocyte/neuron communication (9, 10), and pressure regulation in the eye (11).

Inside cells, cAMP levels are determined by the opposing actions of ACs and cyclic nucleotide-degrading phosphodiesterases. Although phosphodiesterases are widely used as therapeutic targets (12), only a little progress has been made in developing AC-targeting drugs (13). Most of the few AC modulators that are available lack potency, specificity, or pharmacologically favorable properties (3, 14). Among the challenges hindering development of selective AC modulators are the similarities among the catalytic cores of different isoforms and a dearth of structural data (3). At present, only crystal structures for catalytic cores of an artificial AC5/AC2 heterodimer and, more recently, human sAC are available (3, 15, 16). These structures confirmed the general Class III catalytic core architecture with a dimer of identical or structurally closely related domains and the catalytic site formed at the dimer interface (3). In pro-

* This study was supported by Deutsche Forschungsgemeinschaft Grant STE1701/11 (to C. S.) and National Institutes of Health Grants GM107442 and EY025810 (to L. R. L. and J. B.). Drs. Buck and Levin own equity interest in CEP Biotech, which has licensed commercialization of a panel of monoclonal antibodies directed against sAC. All other authors declare that they have no conflicts of interest with the contents of this article. The content is solely the responsibility of the authors and does not necessarily represent the official views of the National Institutes of Health.

The atomic coordinates and structure factors (code 5D0R) have been deposited in the Protein Data Bank (http://wwpdb.org/).

[1] Present address: Dept. of Structural Biology, Stanford University, Stanford, CA 94305.

[2] To whom correspondence should be addressed: Dept. of Biochemistry, University of Bayreuth, Universitaetsstrasse 30, 95447 Bayreuth, Germany. Tel.: 49-921-557831; Fax: 49-921-557832; E-mail: clemens.steegborn@uni-bayreuth.de.

[3] The abbreviations used are: AC, adenylyl cyclase; tmAC, transmembrane adenylyl cyclase; sAC, soluble adenylyl cyclase; HCP, hexachlorophene; DIDS, 4,4′-diisothiocyano-2,2′-stilbenedisulfonic acid; ApCpp, α,β-methylene-ATP; ASI-8, (4-aminofurazan-3-yl)-[3-(1*H*-benzoimidazol-2-ylmethoxy)phenyl]methanone; BBS, bicarbonate binding site; sAC-cat, sAC catalytic domains; r.m.s.d., root mean square deviation.

karyotes, many Class III ACs are active as homodimers of identical domains featuring two symmetric active sites. In contrast, in mammalian tmACs and sAC, two related but non-identical catalytic domains are found in tandem on a single polypeptide chain, resulting in two asymmetric sites (4). The active site features a set of conserved Class III catalytic residues, whereas the second site is degenerate and appears to have evolved into a regulatory pocket (3). In sAC, this site mediates specific activation by bicarbonate, whereas the corresponding site in tmAC allows stimulation by the plant terpene forskolin (4, 17). As a regulatory site for physiological and pharmacological activators, it is a particularly interesting target site for drug development.

Despite the attractiveness of the pseudosymmetric regulatory site, most molecularly characterized AC inhibitors bind to the active site. A widely used class of inhibitors related to the substrate ATP, referred to as P-site inhibitors, exhibits low isoform specificity and likely also affects other nucleotide-binding proteins. The same applies to other compounds based on nucleosides or analogs such as adenine linked to ion chelators and fluorophore-modified nucleotides (3). Compounds binding to a largely hydrophobic pocket next to the active site exhibit some selectivity toward sAC relative to tmACs (18, 19), but the available compounds targeting this site are not suitable as pharmacological drugs. To date, only two classes of compounds are known to modulate ACs via the pseudosymmetric regulatory site: forskolin-related compounds, which modulate tmACs and exhibit some isoform selectivity (14), and the sAC inhibitor (4-aminofurazan-3-yl)-[3-(1*H*-benzoimidazol-2-ylmethoxy)phenyl]methanone (ASI-8), which was recently developed by fragment-based screening (20). ASI-8 has a reported IC_{50} for sAC in the low micromolar range, and it extends from the regulatory site toward the active site where it would clash with substrate (3), suggesting a competitive inhibition mechanism. However, ASI-8 remains to be characterized with respect to kinetic mechanism, isoform selectivity, and suitability for use in cellular systems.

The organochlorine hexachlorophene (HCP) has a wide range of effects such as bacteriostatic activity and inhibition of the Wnt/β catenin pathway (21). It was also reported to inhibit a mammalian AC activity (22), but conflicting results reported in another AC study (23) suggested potential isoform-specific effects. In an effort to identify novel scaffolds for the development of isoform-specific AC inhibitors, we tested whether HCP and bithionol (see Fig. 1*A*), a closely related bioactive organochlorine, might inhibit sAC. We found that both HCP and bithionol are potent inhibitors of human sAC. Biochemical characterization and crystal structure analysis show that bithionol binds to the sAC bicarbonate binding site, revealing new insights in allosteric AC regulation and identifying new leads for drug development.

Experimental Procedures

Chemicals—All chemicals were obtained from Sigma unless otherwise stated.

Protein Production and Purification—A protein construct comprising the human sAC catalytic domains (sAC-cat; residues 1–469) and a C-terminal His_6 tag was expressed in Hi5 insect cells as described (24). The protein was purified through nickel affinity chromatography followed by anion exchange and size exclusion chromatography as described in detail (24). The sAC-cat-R176A variant and a corresponding wild-type protein were expressed as GST fusions in Hi5 cells as described (15).

Crystal Structure Determination of sAC Complexes—Human sAC-cat was crystallized in apo form in hanging drops at 4 °C as described (15). After 5 days, crystals were soaked in drops of cryosolution containing 100 mM sodium acetate, pH 4.8, 200 mM trisodium citrate, 18% (w/v) PEG 4000, 20% (v/v) glycerol, and 20 mM ligand for 2 h at 4 °C. Subsequently, crystals were flash frozen in liquid nitrogen.

Complete data sets for the crystals with space group $P6_3$ were collected at 100 K at the Berlin Electron Storage Ring Society for Synchrotron Radiation beamline 14.1 (BESSY BL14.1) operated by Helmholtz-Zentrum Berlin (25). All diffraction data were processed with XDSAPP (26). The resolution limit of the data set was automatically set by XDSAPP based on CC* (27). Molecular replacement was done with Molrep (28) using the apo structure of sAC (Protein Data Bank code 4CLF) as a search model. Manual model building was done in Coot (29), and refinement was done in Refmac (30). Model quality was analyzed in Coot, and structure figures were generated in PyMOL (Schrödinger, LLC, New York).

Binding Measurements—The bithionol binding affinity was determined by measuring microscale thermophoresis on a Monolith NT.LabelFree instrument (Nanotemper Technologies, Munich, Germany) with 25% UV-light-emitting diode setting and 40% IR laser power. A concentration of 0.4 μM sAC-cat protein was used in 50 mM Tris/HCl, pH 8, 50 mM NaCl, and 15 mM $CaCl_2$. The K_D value was determined twice in independent experiments. Binding transitions were fitted with a single site equation in GraFit (Erithacus Software, East Grinstead, UK).

Activity Measurements—Activity assays were done with 100 ng of purified sAC-cat protein in 50 mM Tris/HCl, pH 8.0, 50 mM NaCl, 10 mM $MgCl_2$, 10 mM $CaCl_2$, and 5 mM ATP at 37 °C. Reactions were stopped by flash freezing. Protein was denatured by heating to 95 °C or by addition of 2% SDS. cAMP produced was measured either as [^{32}P]cAMP as described previously (31), via RapidFire (Agilent, Santa Clara, CA) mass spectrometry or by reversed phase chromatography. For reversed phase chromatography, samples diluted 1:1 with 40 mM ammonium acetate, pH 4.5, were analyzed on a UPLC system (Waters, Milford, MA) with a C_{18} column (Kinetex EVO, Phenomenex; 5 μm, 2.1 × 150 mm) in 97% 20 mM ammonium acetate, pH 4.5, and 3% acetonitrile. cAMP eluted after 1.2 min at a flow rate of 1.0 ml/min. Signal areas were integrated with Empower software (Waters). Measurements were performed in duplicate, and data shown are representatives of at least two repetitions. For fitting of inhibition data at varying inhibitor concentrations, we used a mixed inhibition model where inhibitor binds to apoenzyme with affinity K_i and to a substrate complex with $\alpha \times K_i$ and with both binding events causing complete inhibition. Fitting was done in GraphPad Prism (GraphPad Software, La Jolla, CA) using the following equation.

$$v = \frac{v_{max} \times [S]}{[S] \times \left(1 + \frac{[I]}{\alpha \times K_i}\right) + K_m \times \left(1 + \frac{[I]}{K_i}\right)} \quad \text{(Eq. 1)}$$

cAMP accumulation assays in cultured cells were performed as described (32). Briefly, cellular cAMP was quantitated using the Correlate-EIA Direct cAMP assay (Enzo Life Sciences, Farmingdale, NY) after cellular phosphodiesterases were inhibited with isobutylmethylxanthine (500 μM) for the indicated time.

Results

Bithionol and HCP Are Potent sAC Inhibitors—Because of its variability at inhibiting AC activity in cell lysates (22), we hypothesized that HCP might be an isoform-selective AC inhibitor. We thus tested HCP and the closely related bithionol (Fig. 1*A*) for effects on the activity of purified human sAC-cat protein (residues 1–469). Both substances potently inhibited sAC, and dose-response experiments yielded IC_{50} values of 1.6 ± 0.1 μM for HCP and 4.0 ± 0.2 μM for bithionol (Fig. 1*B*). Thus, these compounds inhibit sAC with similar potencies as ASI-8, the most potent sAC inhibitor identified to date, and KH7, a widely used, highly sAC-specific compound (3).

Inhibition Is Mostly Non-competitive with ATP—Because HCP is an aggressive substance with pleiotropic effects, potentially including membrane disruption and protein denaturation, we tested whether concentrations of HCP capable of fully inhibiting sAC affected the structural integrity of the enzyme. Thermal denaturation of sAC-cat in the presence of 1 or 10 μM HCP did not differ significantly from denaturation of the enzyme in the absence of the compound (Fig. 1*C*). Thus, HCP was not inhibiting sAC by disrupting its structural integrity. Nevertheless, because it has less aggressive chemical properties, we used bithionol to further investigate the mechanism of sAC inhibition. Analyzing the binding of bithionol to apo-sAC through thermophoresis measurements yielded a K_D of 0.43 ± 0.06 μM (Fig. 1*D*), revealing a binding affinity 10-fold stronger than its inhibition potency in activity assays (see above). To further analyze this potential substrate competition, we performed ATP titrations at varying inhibitor concentrations. They revealed a significant decrease of the apparent v_{max} with increasing bithionol concentrations and a weaker increasing effect on the substrate K_m (v_{max}^{app} (nmol/min) and K_m (mM): 58.4 and 0.35 (0 μM bithionol), 52.2 and 0.39 (1.95 μM), 42.8 and 0.64 (7.8 μM), and 6.0 and 0.21 (31.25 μM); the K_m at 31.25 μM bithionol is inaccurate due to the low activity). Thus, as also illustrated by the Lineweaver-Burk transformation of these data (Fig. 1*E*), bithionol acts as a mixed-type inhibitor on sAC. Directly fitting the inhibition data with a mixed model (*i.e.* where inhibitor binds to apoenzyme with affinity K_i and to enzyme·substrate complex with $\alpha \times K_i$) agreed well with the measured data (Fig. 1*F*) and yielded an α factor of 1.7. Thus, bithionol and substrate can bind concomitantly, but they will decrease each other's affinity for sAC. This decreased affinity for bithionol in the presence of ATP likely contributes to the discrepancy between K_d (Fig. 1*D*) and IC_{50} (Fig. 1*B*; the 4.0 μM IC_{50} then corresponds to a K_i of 2.3 μM). The remaining discrepancy indicates an incomplete inhibition model; as described below, bithionol affinity for sAC can also be diminished by other components of the activity assay (*i.e.* bicarbonate). However, our data reveal that although bithionol has a small competitive effect it inhibits sAC mostly through a non-competitive mechanism, indicating that it exploits an allosteric site.

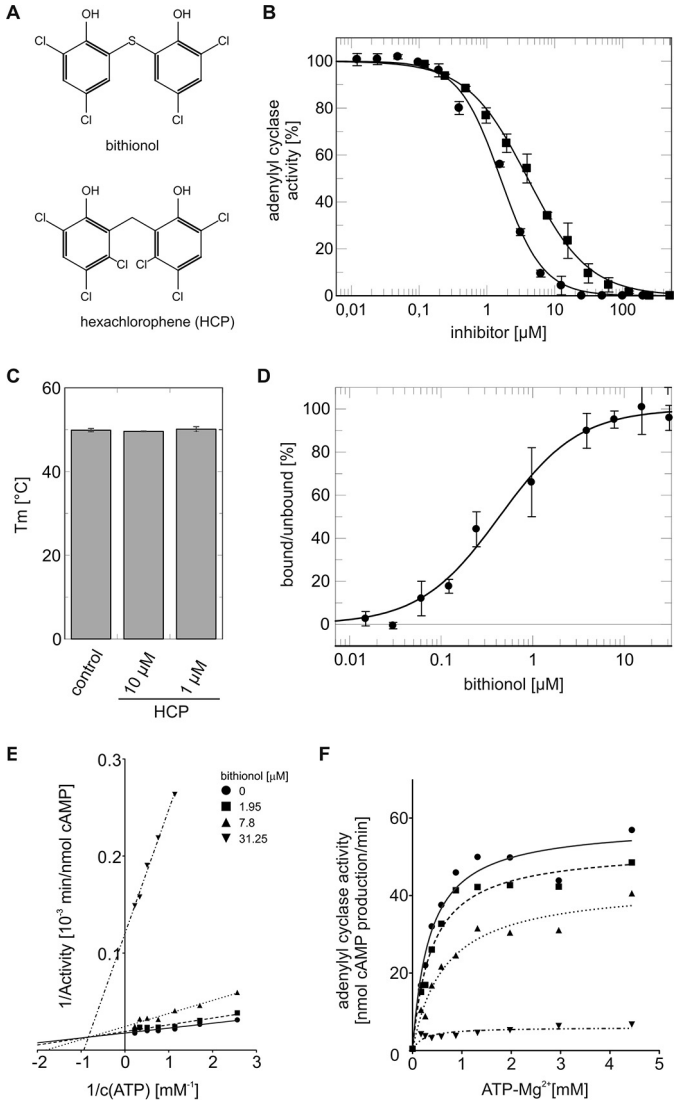

FIGURE 1. **Compound structures and effects on sAC activity.** *A*, chemical structure of bithionol and HCP. *B*, dose-response experiments for HCP (*circles*) and bithionol (*squares*) in the presence of 5 mM ATP and 10 mM $CaCl_2$/$MgCl_2$, resulting in an IC_{50} of 1.6 ± 0.10 μM for HCP and 4.0 ± 0.2 μM for bithionol. *C*, comparison of melting temperatures (T_m) in absence and presence of 10 μM and 1 μM HCP. *D*, binding affinity of bithionol to sAC determined by microscale thermophoresis results in a K_D of 0.43 ± 0.06 μM (*error bars*, S.D.; $n = 2$). *E*, Lineweaver-Burk plot of the inhibition data in *F*, which indicates a mixed-type inhibition. *F*, substrate titrations (in the presence of 10 mM $MgCl_2$, 10 mM $CaCl_2$, and 40 mM $NaHCO_3$) at various bithionol concentrations (*circles*, 0 μM; *squares*, 1.95 μM; *triangles*, 7.8 μM; *upside-down triangles*, 31.25 μM). The curves show a fit to a mixed-type inhibition model.

Bithionol Blocks the Activator Binding Site and Its Entrance—To identify the molecular details of this allosteric binding site and inhibition mechanism, we solved a crystal structure of an sAC·inhibitor complex. In soaking experiments with HCP, sAC apo crystals cracked and dissolved possibly due to a compound effect on the protein conformation (see "Discussion"). In contrast, after soaking sAC apo crystals with bithionol, we were able to collect diffraction data to 2.24-Å resolution (Table 1).

TABLE 1
Diffraction data and refinement statistics
Values in parentheses refer to the highest resolution shell. CC, cross-correlation.

	sAC·bithionol
Data collection	
Space group	$P6_3$
Unit cell constants	$a = b = 99.4$ Å, $c = 100.0$ Å; $\alpha = \beta = 90°$, $\gamma = 120°$
Wavelength (Å)	0.918
Resolution (Å)	86.23–2.24
Total reflections	137,147 (22,232)
Unique reflections	27,051 (4,321)
Multiplicity	5.1 (5.1)
$I/\sigma I$	11.9 (1.7)
Completeness (%)	100 (99)
$CC_{1/2}$	100 (56)
R_{meas}[a] (%)	15.4 (99.6)
Refinement	
Refinement resolution (Å)	2.24
Reflections	25,668
R[b]/R_{free}[c] (%)	17.7/24.4
Protein atoms	3,668
Solvent atoms	233
Ligand atoms	19
r.m.s.d.	
Bond lengths (Å)	0.02
Bond angles (°)	1.97
Ramachandran plot	
Preferred region (%)	95.8
Additionally allowed region (%)	4.2
Disallowed region (%)	0
Average B-factor (Å^2)	36.5
Protein (Å^2)	36.2
Solvent (Å^2)	39.2
Ligand (Å^2)	42.0

[a] $R_{meas} = (\Sigma_h \sqrt{n/(n-1)}\Sigma|\langle I\rangle - I|)/(\Sigma_h \Sigma I)$ where I is the intensity of an individual measurement, $\langle I\rangle$ is the corresponding mean value, and h and n are the indices and redundancies of the reflections.
[b] R-factor $= R = (\Sigma_{hkl}||F_{obs}| - k|F_{calc}||)/(\Sigma_{hkl}|F_{obs}|)$ where $|F_{obs}|$ is the observed and $|F_{calc}|$ is the calculated structure factor amplitude.
[c] R_{free} was calculated from 5% of measured reflections omitted from refinement.

Molecular replacement phasing with apo-sAC as a search model yielded additional electron density fitting to bithionol. Building in bithionol and refining the structure resulted in an sAC·bithionol complex with well defined ligand geometry and excellent refinement statistics (Fig. 2, *A* and *B*, and Table 1; R_{cryst}/R_{free} = 17.8/24.6%). The ligand occupies the previously identified bicarbonate binding site (BBS) (3, 15) as well as the channel connecting this regulatory site to the active site (Fig. 2*C*). An average B-factor for bithionol of 42 Å^2, which fits well to the average B-factor of the environment (36 Å^2), indicates that the inhibitor is tightly bound, consistent with the measured high affinity. The inhibitor is mainly bound (Fig. 2*D*) through hydrophobic interactions with Val^{167}, Ala^{100}, Leu^{162}, Leu^{102}, and Val^{175}. In addition, the bithionol aromatic ring systems bind to a hydrophobic patch formed by Phe^{338}/Phe^{296}, and to Phe^{45} and Phe^{336} through T-shaped π-stacking interactions. The hydroxyl group of the bithionol ring oriented into the BBS forms a hydrogen bond to the backbone amide of Met^{337}. The chlorine functions of bithionol also appear to form several polar interactions to the side chain of Lys^{95}, to the backbone amide of Val^{167} and possibly to the carbonyl oxygens of Ala^{100} and Leu^{162} and to a water molecule. Arg^{176}, a residue suggested to act as a trigger flipping between active site and BBS (15), is oriented vertically to one of the bithionol aromatic rings. With a distance of about 4 Å, it appears to interact with the bithionol π-electrons. Consistent with an Arg^{176} contribution to inhibitor binding, bithionol inhibition of an sAC-cat-R176A mutant required 2–3-fold higher inhibitor concentrations than wild-type sAC-cat (Fig. 2*E*).

Bithionol binds deeply into the sAC BBS (Fig. 2*C*). A bithionol chlorine is positioned within 0.8 Å from the position of the bicarbonate carbon atom in the sAC·bicarbonate complex. Both ligands should thus compete for the BBS. As a first test, we performed bithionol titrations at increasing bicarbonate levels. Adding bicarbonate shifted the inhibition curve to the right, *i.e.* to higher IC_{50} values (Fig. 2*F*), consistent with a competition between bicarbonate and bithionol. However, mechanistic details of this complex system such as direct *versus* indirect competition remain to be analyzed.

An Allosteric Inhibition Mechanism for Bithionol—In the sAC·bithionol complex, the ligand fills the BBS and the narrow channel connecting the BBS to the active site (Fig. 2*C*). Comparison with the published structure of sAC in complex with the substrate analog ApCpp (Protein Data Bank code 4CLK) (15) reveals that bithionol almost reaches the ATP substrate binding site but would not significantly overlap with it (Figs. 2*C* and 3*A*). At their closest, a bithionol hydroxyl group would come within ~2.7 Å of the 2′-OH of the ribose in the substrate ATP. This relatively minor direct clash is consistent with the mostly non-competitive inhibition observed in activity assays (Fig. 1, *E* and *F*; see above). However, our attempts to soak bithionol into sAC·ApCpp complexes failed to yield significant density for the inhibitor, agreeing with the observation that bithionol inhibition also has a competitive component and thus that both ligands do not bind entirely independently.

Comparing the sAC·bithionol complex with apo-sAC and other sAC·ligand complexes revealed conformational differences that suggest a mechanism for the inhibitory effect of this ligand. Phe^{338} and Phe^{336} are moved slightly closer to the ATP adenosine binding site in the bithionol complex (Fig. 3*A*). This movement seems to tighten the substrate binding site. Striking changes in the bithionol complex are also found in and around the catalytic $\beta2$-$\beta3$ loop. Although the $\beta2$-$\beta3$ loop from the second catalytic domain (C2), which contributes to the BBS, is in a position similar to its position in the sAC·ApCpp complex, the catalytic $\beta2$-$\beta3$ loop of the first catalytic domain (C1) is in an inactive conformation. The density for the loop residue Asp^{99}, which is one of the two conserved Asp residues binding the two catalytically essential divalent ions, is not well defined. This lack of order appears to be due to the bithionol ligand. Bicarbonate-dependent sAC activation involves a "flipping" away of Arg^{176} from Asp^{99}. In the apo state, Arg^{176} forms a salt bridge with Asp^{99}, whereas in the bicarbonate-activated state, Arg^{176} assumes an "activation position" that frees Asp^{99} to be appropriately positioned with Asp^{49} to form two binding sites for the divalent ions in the substrate complex (15). In the sAC·bithionol structure, Arg^{176} is oriented similarly to the sAC·bicarbonate complex but shifted away from the BBS to provide space for the inhibitor (Fig. 3*B*). In fact, the Arg^{176} side chain interacts significantly with the inhibitor and contributes to its binding affinity (see above). Because of the altered Arg^{176} orientation and associated smaller active site rearrangements, Asp^{99} appears to be flexible but positioned too close to Asp^{49} for ion site formation. The Asp^{99}-Asp^{49} distance is 2.8 Å due to a shift of the region spanning from Asp^{47} to Ala^{53}. In particular,

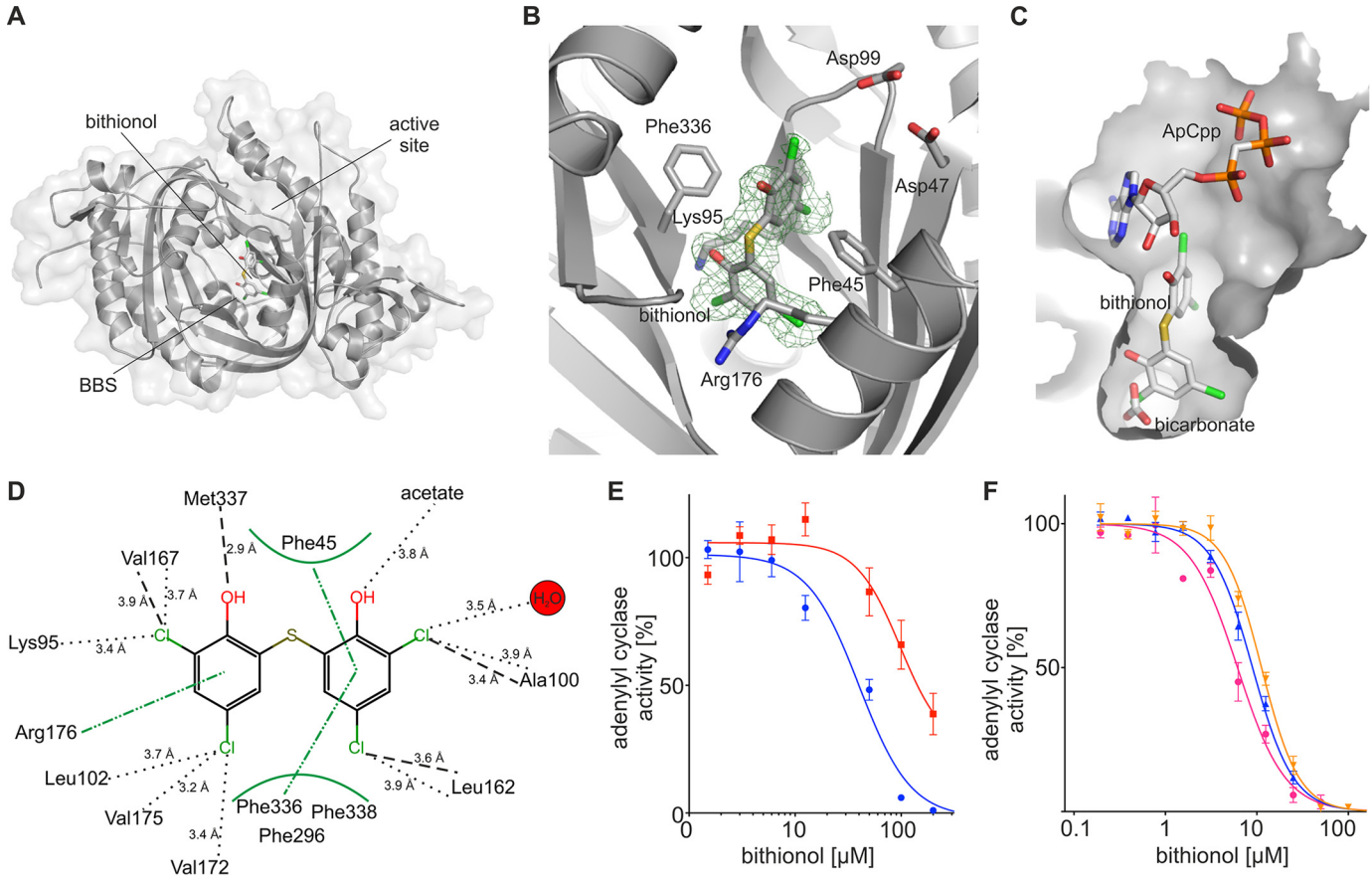

FIGURE 2. **Crystal structure of an sAC·bithionol complex.** *A*, overall structure of the sAC·bithionol complex in backbone representation with bithionol displayed as *sticks*. *B*, bithionol in *stick* representation overlaid with $F_o - F_c$ omit electron density (*green*) contoured at 2.5σ. Several interacting residues are shown as *sticks* colored according to atom type. *C*, surface of active site and inhibitor-containing BBS of the sAC·bithionol complex overlaid with bicarbonate from an sAC·bicarbonate complex and ApCpp from an sAC·ApCpp complex. Protein is shown as *gray surface*, and all ligands are in *stick* representation colored according to atom type. *D*, interaction scheme for the sAC·bithionol complex. Interactions to side chains are indicated by *black dots*, backbone interactions are indicated with *dashed lines*, and interactions with the aromatic ring systems are indicated with *green broken lines*. *E*, dose-response relationships for bithionol inhibition of wild-type human sAC (*blue circles*) and an sAC-R176A mutant (*red squares*) assayed in the presence of 1 mM ATP, 5 mM $MgCl_2$, 5 mM $CaCl_2$, and 30 mM $NaHCO_3$. Data points are normalized to the activity in the absence of bithionol (*error bars*, S.E.; $n = 3$; absolute basal activity: wild type, 44.1 nmol/min; mutant, 8.6 nmol/min). *F*, bithionol inhibition appears to be competitive with bicarbonate. Dose-response relationships for bithionol inhibition of wild-type human sAC assayed in the presence of 1 mM ATP, 5 mM $MgCl_2$, 5 mM $CaCl_2$, and no $NaHCO_3$ (*magenta circles*; absolute basal activity, 13.6 nmol/min) or in the presence of 20 mM (*blue triangles*; absolute basal activity, 55.4 nmol/min) or 40 mM (*orange inverted triangles*; absolute basal activity, 63.1 nmol/min) $NaHCO_3$ (*error bars*, S.E.; $n = 3$) are shown. Data points are normalized to the respective basal activity in the absence of bithionol, and each titration was fitted individually with a standard inhibitor binding model (IC_{50} values, 6 (no bicarbonate), 9 (20 mM bicarbonate), and 11 μM (40 mM bicarbonate)).

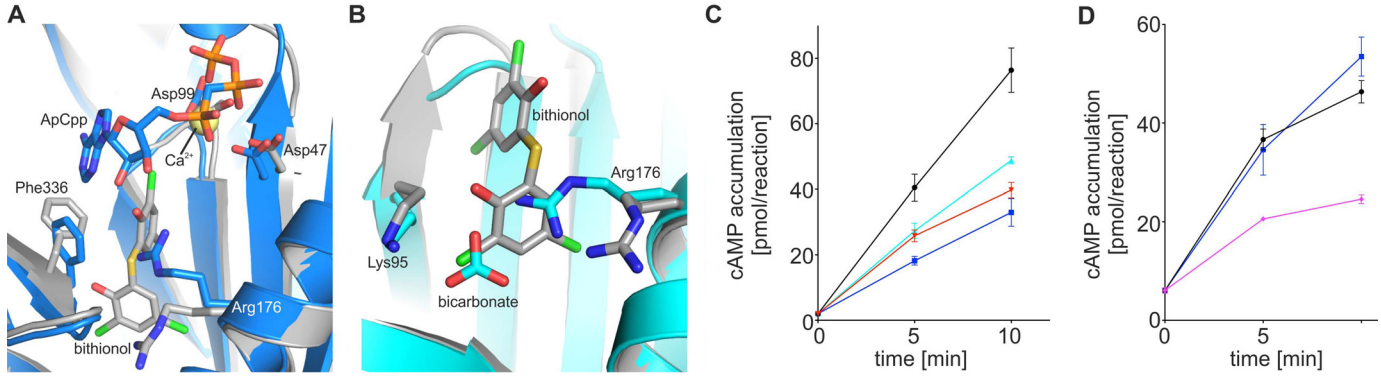

FIGURE 3. **Comparison of the sAC·bithionol complex with other sAC conformations and analysis of cellular bithionol effects and selectivity.** *A*, overlay of the sAC·bithionol complex (*gray*) with an sAC·ApCpp complex (*blue*; r.m.s.d., 0.6 Å for 407 Cα atoms). ApCpp, bithionol, and relevant amino acid side chains are shown in *stick* representation and colored according to atom type (carbon atoms colored as the corresponding protein). Ca^{2+} is shown as a *yellow sphere*. *B*, overlay of the sAC·bithionol complex with an sAC·bicarbonate complex structure (*cyan*; r.m.s.d., 0.4 Å for 356 Cα atoms). Bithionol, bicarbonate, and relevant amino acid side chains are shown in *stick* representation and colored according to atom type. *C*, time course of cAMP accumulation in sAC-overexpressing 4-4 cells in the absence of inhibitor (*black circles*) or in the presence of 50 μM bithionol (*cyan triangles*), 100 μM bithionol (*blue squares*), or 30 μM KH7 (*red inverted triangles*; *error bars*, S.E.; $n = 3$). *D*, time course of cAMP accumulation in sAC KO mouse embryonic fibroblasts in the presence of 50 μM forskolin and no inhibitor (*black circles*), 100 μM bithionol (*blue squares*), or 50 μM 2′,5′-dideoxyadenosine (*magenta diamonds*; *error bars*, S.E.; $n = 3$).

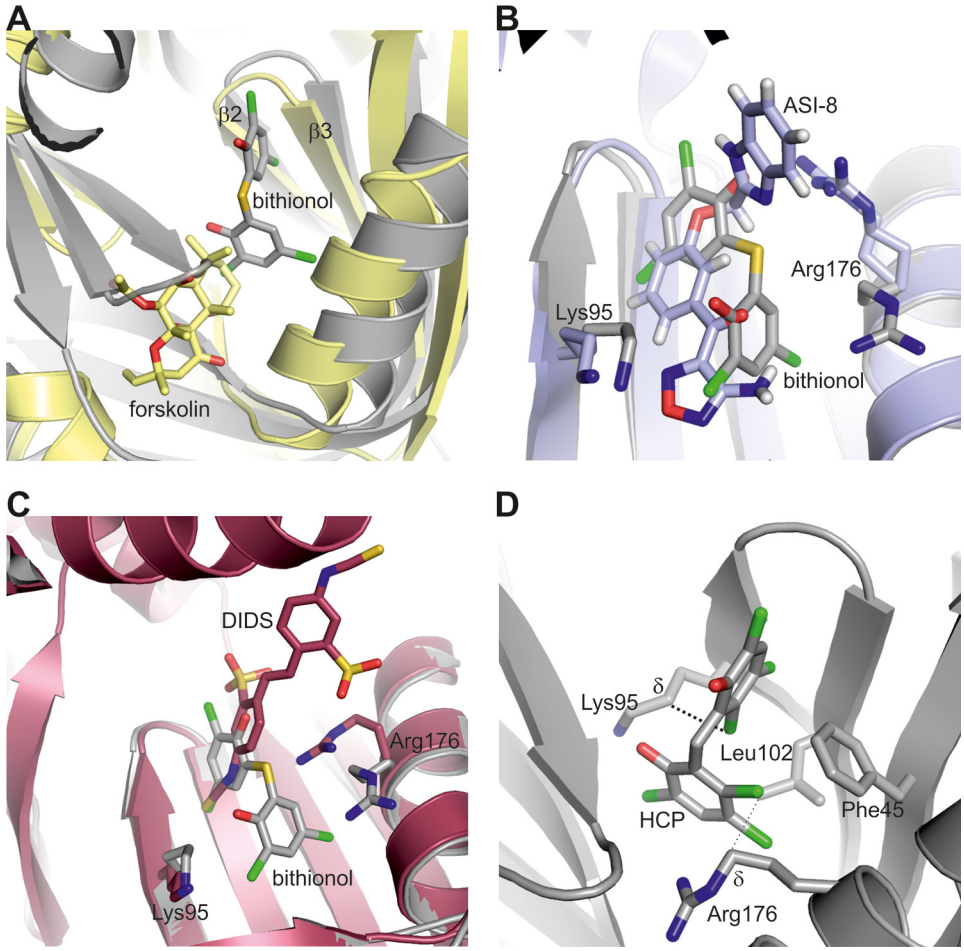

FIGURE 4. **Comparison of the sAC·bithionol complex with other sAC·inhibitor complexes.** *A*, overlay of sAC·bithionol (*gray*) with a tmAC·forskolin complex structure (*yellow*; r.m.s.d., 8.7 Å for 227 Cα atoms) with bithionol and forskolin in *stick* representation. *B*, overlay of the sAC·bithionol complex (*gray*) with an sAC·ASI-8 complex (*light blue*; r.m.s.d., 0.3 Å for 382 Cα atoms). Inhibitors and relevant amino acid side chains are shown in *stick* representation. *C*, overlay of sAC·bithionol (*gray*) with an sAC·DIDS complex structure (*red*; r.m.s.d., 0.4 Å for 403 Cα atoms). DIDS mainly occupies the entrance region to the active site and BBS. Both inhibitors and relevant residue side chains are shown in *stick* representation. *D*, modeling of HCP into the bithionol position of the sAC·bithionol structure. HCP and nearby amino acid side chains are shown as *sticks* colored according to atom type. The *dotted lines* indicate distances between protein and the additional chlorines in HCP discussed in the text.

Thr[52], which usually interacts with the γ-phosphate of the substrate ATP, is shifted and rotates ~3 Å away. These active site rearrangements induced by bithionol binding to the BBS likely hinder formation of a productive sAC complex with catalytic ions and ATP.

Bithionol Is Active in Cellular Systems and Specific for sAC Relative to tmACs—We analyzed adenylyl cyclase activity in cellular systems by inhibiting phosphodiesterase activity and allowing cAMP to accumulate. To test whether our allosteric inhibitor bithionol can modulate sAC activity *in vivo*, we tested its effect on cAMP accumulation in cultured 4-4 cells, which stably overexpress sAC (33). As we showed previously (32, 33), the majority of cAMP accumulating in these 4-4 cells is produced by sAC. Similarly to the widely used sAC-specific inhibitor KH7, bithionol caused a dose-dependent decrease in cAMP formation with essentially complete inhibition of sAC-dependent cAMP accumulation at 100 μM (Fig. 3*C*). Because bithionol exploits the unique bicarbonate site of sAC, we predicted it would be specific for sAC relative to tmACs. To analyze its effects on tmAC-dependent cAMP formation, we tested whether bithionol inhibited forskolin-stimulated cAMP accumulation in sAC KO mouse embryonic fibroblasts, which exclusively reflects tmAC activity (32). As expected, forskolin-stimulated cAMP accumulation in sAC KO mouse embryonic fibroblasts was inhibited by the tmAC-specific P-site inhibitor 2′,5′-dideoxyadenosine (32), whereas bithionol did not inhibit this tmAC-dependent cAMP accumulation at concentrations up to 100 μM (Fig. 3*D*). Thus, bithionol is an sAC-specific AC inhibitor in cellular contexts.

Discussion

Few potent inhibitors are currently available for sAC, a potential target, *e.g.* for contraception (34) and for therapy of diabetes (35), ocular hypotony, and glaucoma (11). We describe here that the bisphenol bithionol inhibits human sAC potently and specifically by exploiting an allosteric mechanism via the bicarbonate regulation site of the enzyme. The corresponding site in mammalian tmACs serves as the binding site for the non-physiological, tmAC-specific activator forskolin (3, 36). Comparing the sAC·bithionol and tmAC·forskolin (Protein Data Bank code 1CJT (36) complexes illustrates the molecular differences causing the sAC specificity of bithionol (Fig. 4*A*). In

sAC, the inhibitor fills the BBS and its entrance almost completely. In contrast, the tmAC forskolin site is significantly extended compared with the BBS; it would fail to provide an appropriately sized binding pocket for bithionol, resulting in insufficient interactions for high affinity binding. In fact, the forskolin and bithionol binding sites hardly overlap (Fig. 4*A*). The extended $\beta2$-$\beta3$ loop in sAC tightens the BBS and prevents access to most of the region corresponding to the tmAC forskolin site. This tightening of the regulatory site in sAC prevents forskolin binding to sAC and provides binding interactions for bithionol, which make the inhibitor sAC-specific.

Bithionol is the first known sAC inhibitor that acts through the BBS and via a mostly non-competitive, allosteric mechanism. Allosteric activation of tmACs by forskolin binding to the analogous regulatory site appears to be mediated via stabilization of an active orientation of the catalytic domains (C1 and C2) (37). Bithionol does not seem to have a significant effect on the relative orientation of sAC C1 and C2 domains, and such a domain reorientation also does not appear to be relevant for the bicarbonate-dependent sAC activation mediated by this site (15). Instead, binding of bicarbonate and of bithionol involves major rearrangements of residues relevant for productive substrate binding and for communication between active and regulatory sites. A key residue for this communication is Arg^{176}, which assumes a unique conformation in the sAC·bithionol complex. Arg^{176} forms a salt bridge with the catalytic Asp^{99} in the inactive sAC apo state, reorients toward the ATP 2′-OH in an sAC·substrate complex, and turns away from the active site for interaction with bicarbonate in the BBS in the stimulated sAC state (Fig. 3, *A* and *B*) (15, 38). Although the mechanistic role of Arg^{176} is not fully understood, its rearrangements are clearly implicated in sAC catalysis and, in particular, in sAC activation (15). And shown here, Arg^{176} is involved in bithionol inhibition. The Arg^{176}/bithionol interaction appears to provide binding energy and causes a unique side-chain conformation oriented away from the active site and displaced from its activation position (Fig. 3*B*). Together with the associated rearrangements of the catalytic Asp residues, which prevent binding of the catalytic metal ions, the reorientation of Arg^{176} appears to contribute to the allosteric mechanism leading to sAC inhibition. However, an sAC-R176A mutant is inhibited by bithionol, albeit with lower potency, and inhibition also appears to have a competitive component. The lower potency likely reflects the loss of interaction energy between the Arg and bithionol. The competition could stem from a direct clash with the substrate ribose, although the exact position of the ATP sugar in a productive substrate complex can only be estimated based on the available structures (15, 38). Another contribution to a lower substrate affinity in the presence of bithionol could come from the restriction of the adenosine binding site caused by the bithionol-induced reorientation of Phe^{336}.

A previously described sAC inhibitor occupying the BBS is ASI-8, the compound with the most potent effect on sAC (IC_{50} $\sim$ 0.4 μM) described thus far (20). ASI-8 is a longer molecule than bithionol, however, and it extends out of the BBS (and the connecting channel) into the substrate binding site (Fig. 4*B*). No data are available for the specificity or mechanism of ASI-8 inhibition, but comparisons of the respective crystal structures predict that ASI-8 would severely clash, and thus compete, with the substrate ATP. ASI-8 was developed by fusing smaller fragments, and a subset of the smaller precursors showed BBS binding and very weak sAC inhibition. Because these smaller fragments do not block the substrate site, they may be allosteric inhibitors similar to bithionol. An inhibitor class using a related mechanism but mostly another binding site than bithionol are catechol estrogens (19). They bind to a central surface of the catalytic dimer and orient their catechol moiety toward the catalytic ions and the substrate phosphates. Through a direct, strong interaction with ion A, they interfere with proper ion positioning and with the ATP conformation required for turnover (19).

Bithionol and HCP appear to affect a number of targets and have pleiotropic biological effects from antiviral and antibacterial activity to inhibition of cancer cell growth. In fact, bithionol is used as an antiparasitic agent in animals and was used as an antibacterial agent in cosmetics until this application was prohibited by the Food and Drug Administration because of its photosensitizing effect. Bithionol also showed little specificity in its cytotoxic effect on a panel of ovarian cancer cell lines (39), and we found general cytotoxic effects starting around 10 μM (data not shown), *i.e.* at concentrations that would be required for significant sAC inhibition *in vivo*. Therefore, bithionol and HCP themselves appear unsuitable as drugs. However, the binding site, inhibition mechanism, and chemical scaffold can serve as starting points for the development of more specific sAC inhibitors. Another sAC inhibitor binding to a bithionol-related region is 4,4′-diisothiocyano-2,2′-stilbenedisulfonic acid (DIDS) (15). DIDS is known as a blocker of bicarbonate channels and inhibits sAC weakly. It binds to the entrance shared by the sAC active site and its BBS, blocking access for substrate as well as activator (Fig. 4*C*) (15). Its binding site overlaps partially with the bithionol site, exploiting the same hydrophobic patch formed by $Phe^{45/336/338}$. Being smaller than DIDS, bithionol is positioned more deeply in the BBS, whereas DIDS extends further to the active site entrance of the catalytic core (Fig. 4*C*). Although DIDS shows limited sAC affinity, it illustrates the possibility to extend BBS ligands toward the active site entrance for increased interaction interfaces, affinity, and potency. Together, these observations suggest that adding moieties that mimic the interactions observed in the sAC complexes with ASI-8 (20) and DIDS (15) may improve HCP/bithionol derivatives.

Understanding why HCP was more potent than the closely related bithionol might also be helpful for future development of sAC inhibitors based on this scaffold. Because no experimental sAC·HCP complex structure could be obtained, we modeled the HCP complex based on the sAC·bithionol structure (Fig. 4*D*). One of the additional chlorines found in HCP would point into the pocket between Phe^{45} (2.9 Å) and the side chain of Arg^{176} (δ carbon position, 3.0 Å). The second chlorine atom would point in the direction of Leu^{102} and Lys^{95} (δ carbon position, 3.4 Å). Although we cannot exclude that bithionol and HCP have different inhibition mechanisms as described previously for another target (40), it is tempting to hypothesize that the additional interactions due to the chlorines might cause the slightly higher HCP affinity and potency. The sensitive

response to small compound variations suggests that further modifications of the bithionol/HCP scaffold might enable improving it into a specific sAC inhibitor.

Our work identified HCP/bithionol as potent sAC inhibitors that exploit the unique activator binding site in sAC for an allosteric mechanism of sAC inhibition. The BBS thus serves as a general allosteric sAC regulation site, enabling activation as well as inhibition. Whether there are physiological sAC ligands that exploit this site for inhibition remains to be seen. However, analyzing the allosteric mechanisms of sAC activation and inhibition through BBS ligands helps understanding sAC regulation and provides novel approaches for pharmacological sAC modulation. Our structural analysis of sAC inhibition by bithionol reveals contributing conformational changes and binding details, which provide a rational basis for further development of BBS ligands as potent and specific sAC modulators.

Author Contributions—S. K., L. R. L., J. B., and C. S. designed the research project. S. K., J. v. d. H., H. B., L. C., and L. R.-E. performed experiments. S. K. and C. S. solved the crystal structure. S. K., L. R. L., J. B., J. F. G., and C. S. analyzed data. S. K. and C. S., supported by L. R. L. and J. B., wrote the paper.

Acknowledgments—We thank the Berlin Electron Storage Ring Society for Synchrotron Radiation (BESSY) staff for technical assistance, the Helmholtz Protein Sample Production Facility for support in producing sAC protein, and the Helmsley Trust for funding of the Agilent RapidFire mass spectrometry instrument.

References

1. Kopperud, R., Krakstad, C., Selheim, F., and Døskeland, S. O. (2003) cAMP effector mechanisms. Novel twists for an "old" signaling system. *FEBS Lett.* **546,** 121–126
2. Gancedo, J. M. (2013) Biological roles of cAMP: variations on a theme in the different kingdoms of life: biological roles of cAMP. *Biol. Rev.* **88,** 645–668
3. Steegborn, C. (2014) Structure, mechanism, and regulation of soluble adenylyl cyclases—similarities and differences to transmembrane adenylyl cyclases. *Biochim. Biophys. Acta* **1842,** 2535–2547
4. Kamenetsky, M., Middelhaufe, S., Bank, E. M., Levin, L. R., Buck, J., and Steegborn, C. (2006) Molecular details of cAMP generation in mammalian cells: a tale of two systems. *J. Mol. Biol.* **362,** 623–639
5. Tresguerres, M., Levin, L. R., and Buck, J. (2011) Intracellular cAMP signaling by soluble adenylyl cyclase. *Kidney Int.* **79,** 1277–1288
6. Esposito, G., Jaiswal, B. S., Xie, F., Krajnc-Franken, M. A., Robben, T. J., Strik, A. M., Kuil, C., Philipsen, R. L., van Duin, M., Conti, M., Gossen, J. A., and Jaiswal, B. S. (2004) Mice deficient for soluble adenylyl cyclase are infertile because of a severe sperm-motility defect. *Proc. Natl. Acad. Sci. U.S.A.* **101,** 2993–2998
7. Hess, K. C., Jones, B. H., Marquez, B., Chen, Y., Ord, T. S., Kamenetsky, M., Miyamoto, C., Zippin, J. H., Kopf, G. S., Suarez, S. S., Levin, L. R., Williams, C. J., Buck, J., and Moss, S. B. (2005) The soluble adenylyl cyclase in sperm mediates multiple signaling events required for fertilization. *Dev. Cell* **9,** 249–259
8. Levin, L. R., and Buck, J. (2015) Physiological roles of acid-base sensors. *Annu. Rev. Physiol.* **77,** 347–362
9. Choi, H. B., Gordon, G. R., Zhou, N., Tai, C., Rungta, R. L., Martinez, J., Milner, T. A., Ryu, J. K., McLarnon, J. G., Tresguerres, M., Levin, L. R., Buck, J., and MacVicar, B. A. (2012) Metabolic communication between astrocytes and neurons via bicarbonate-responsive soluble adenylyl cyclase. *Neuron* **75,** 1094–1104
10. Xie, F., Garcia, M. A., Carlson, A. E., Schuh, S. M., Babcock, D. F., Jaiswal, B. S., Gossen, J. A., Esposito, G., van Duin, M., and Conti, M. (2006) Soluble adenylyl cyclase (sAC) is indispensable for sperm function and fertilization. *Dev. Biol.* **296,** 353–362
11. Lee, Y. S., Tresguerres, M., Hess, K., Marmorstein, L. Y., Levin, L. R., Buck, J., and Marmorstein, A. D. (2011) Regulation of anterior chamber drainage by bicarbonate-sensitive soluble adenylyl cyclase in the ciliary body. *J. Biol. Chem.* **286,** 41353–41358
12. Maurice, D. H., Ke, H., Ahmad, F., Wang, Y., Chung, J., and Manganiello, V. C. (2014) Advances in targeting cyclic nucleotide phosphodiesterases. *Nat. Rev. Drug Discov.* **13,** 290–314
13. Pierre, S., Eschenhagen, T., Geisslinger, G., and Scholich, K. (2009) Capturing adenylyl cyclases as potential drug targets. *Nat. Rev. Drug Discov.* **8,** 321–335
14. Seifert, R., Lushington, G. H., Mou, T.-C., Gille, A., and Sprang, S. R. (2012) Inhibitors of membranous adenylyl cyclases. *Trends Pharmacol. Sci.* **33,** 64–78
15. Kleinboelting, S., Diaz, A., Moniot, S., van den Heuvel, J., Weyand, M., Levin, L. R., Buck, J., and Steegborn, C. (2014) Crystal structures of human soluble adenylyl cyclase reveal mechanisms of catalysis and of its activation through bicarbonate. *Proc. Natl. Acad. Sci. U.S.A.* **111,** 3727–3732
16. Tesmer, J. J., Sunahara, R. K., Gilman, A. G., and Sprang, S. R. (1997) Crystal structure of the catalytic domains of adenylyl cyclase in a complex with Gsα·GTPγS. *Science* **278,** 1907–1916
17. Insel, P. A., and Ostrom, R. S. (2003) Forskolin as a tool for examining adenylyl cyclase expression, regulation, and G protein signaling. *Cell. Mol. Neurobiol.* **23,** 305–314
18. Schlicker, C., Rauch, A., Hess, K. C., Kachholz, B., Levin, L. R., Buck, J., and Steegborn, C. (2008) Structure-based development of novel adenylyl cyclase inhibitors. *J. Med. Chem.* **51,** 4456–4464
19. Steegborn, C., Litvin, T. N., Hess, K. C., Capper, A. B., Taussig, R., Buck, J., Levin, L. R., and Wu, H. (2005) A novel mechanism for adenylyl cyclase inhibition from the crystal structure of its complex with catechol estrogen. *J. Biol. Chem.* **280,** 31754–31759
20. Saalau-Bethell, S. M., Berdini, V., Cleasby, A., Congreve, M., Coyle, J. E., Lock, V., Murray, C. W., O'Brien, M. A., Rich, S. J., Sambrook, T., Vinkovic, M., Yon, J. R., and Jhoti, H. (2014) Crystal structure of human soluble adenylate cyclase reveals a distinct, highly flexible allosteric bicarbonate binding pocket. *ChemMedChem* **9,** 823–832
21. Park, S., Gwak, J., Cho, M., Song, T., Won, J., Kim, D. E., Shin, J. G., and Oh, S. (2006) Hexachlorophene inhibits Wnt/β-catenin pathway by promoting Siah-mediated β-catenin degradation. *Mol. Pharmacol.* **70,** 960–966
22. Mavier, P., Stengel, D., and Hanoune, J. (1976) Inhibition of adenylate cyclase and ATPase activities from rat liver plasma membrane by hexachlorophene. *Biochem. Pharmacol.* **25,** 305–309
23. Leow, A. C., Towns, K. M., and Leaver, D. D. (1979) Effect of organotin compounds and hexachlorophene on brain adenosine cyclic 3′,5′-monophosphate metabolism. *Chem. Biol. Interact.* **27,** 125–132
24. Kleinboelting, S., van den Heuvel, J., Kambach, C., Weyand, M., Leipelt, M., and Steegborn, C. (2014) Expression, purification, crystallization, and preliminary x-ray diffraction analysis of a mammalian type 10 adenylyl cyclase. *Acta Crystallogr. F Struct. Biol. Commun.* **70,** 467–469
25. Mueller, U., Darowski, N., Fuchs, M. R., Förster, R., Hellmig, M., Paithankar, K. S., Pühringer, S., Steffien, M., Zocher, G., and Weiss, M. S. (2012) Facilities for macromolecular crystallography at the Helmholtz-Zentrum Berlin. *J. Synchrotron Radiat.* **19,** 442–449
26. Krug, M., Weiss, M. S., Heinemann, U., and Mueller, U. (2012) XDSAPP: a graphical user interface for the convenient processing of diffraction data using XDS. *J. Appl. Crystallogr.* **45,** 568–572
27. Diederichs, K., and Karplus, P. A. (2013) Better models by discarding data? *Acta Crystallogr. D Biol. Crystallogr.* **69,** 1215–1222
28. Vagin, A. A., and Isupov, M. N. (2001) Spherically averaged phased translation function and its application to the search for molecules and fragments in electron-density maps. *Acta Crystallogr. D Biol. Crystallogr.* **57,** 1451–1456
29. Emsley, P., Lohkamp, B., Scott, W. G., and Cowtan, K. (2010) Features and development of Coot. *Acta Crystallogr. D Biol. Crystallogr.* **66,** 486–501
30. Murshudov, G. N., Vagin, A. A., and Dodson, E. J. (1997) Refinement of macromolecular structures by the maximum-likelihood method. *Acta*

Crystallogr. D Biol. Crystallogr. **53,** 240–255
31. Litvin, T. N., Kamenetsky, M., Zarifyan, A., Buck, J., and Levin, L. R. (2003) Kinetic properties of "soluble" adenylyl cyclase: synergism between calcium and bicarbonate. *J. Biol. Chem.* **278,** 15922–15926
32. Bitterman, J. L., Ramos-Espiritu, L., Diaz, A., Levin, L. R., and Buck, J. (2013) Pharmacological distinction between soluble and transmembrane adenylyl cyclases. *J. Pharmacol. Exp. Ther.* **347,** 589–598
33. Zippin, J. H., Chen, Y., Straub, S. G., Hess, K. C., Diaz, A., Lee, D., Tso, P., Holz, G. G., Sharp, G. W., Levin, L. R., and Buck, J. (2013) CO_2/HCO_3^- and calcium regulated soluble adenylyl cyclase as a physiological ATP sensor. *J. Biol. Chem.* **288,** 33283–33291
34. Buffone, M. G., Wertheimer, E. V., Visconti, P. E., and Krapf, D. (2014) Central role of soluble adenylyl cyclase and cAMP in sperm physiology. *Biochim. Biophys. Acta* **1842,** 2610–2620
35. Holz, G. G., Leech, C. A., and Chepurny, O. G. (2014) New insights concerning the molecular basis for defective glucoregulation in soluble adenylyl cyclase knockout mice. *Biochim. Biophys. Acta* **1842,** 2593–2600
36. Tesmer, J. J., Sunahara, R. K., Johnson, R. A., Gosselin, G., Gilman, A. G., and Sprang, S. R. (1999) Two-metal-ion catalysis in adenylyl cyclase. *Science* **285,** 756–760
37. Dessauer, C. W., Scully, T. T., and Gilman, A. G. (1997) Interactions of forskolin and ATP with the cytosolic domains of mammalian adenylyl cyclase. *J. Biol. Chem.* **272,** 22272–22277
38. Kleinboelting, S., van den Heuvel, J., and Steegborn, C. (2014) Structural analysis of human soluble adenylyl cyclase and crystal structures of its nucleotide complexes—implications for cyclase catalysis and evolution. *FEBS J.* **281,** 4151–4164
39. Ayyagari, V. N., and Brard, L. (2014) Bithionol inhibits ovarian cancer cell growth *in vitro*—studies on mechanism(s) of action. *BMC Cancer* **14,** 61
40. Li, M., Smith, C. J., Walker, M. T., and Smith, T. J. (2009) Novel inhibitors complexed with glutamate dehydrogenase: allosteric regulation by control of protein dynamics. *J. Biol. Chem.* **284,** 22988–23000